

## Model of a Permanent Magnet Synchronous Linear Motor for an Urban Transport Electric Vehicle

Mónica Chinchilla Sánchez  
mchin@ing.uc3m.es

Jaime Montoya Larrahondo  
jmlingenieria@gmail.com

Universidad Carlos III de Madrid  
Leganes, Spain

**Abstract** — This work proposes a new linear motor for an electric bus propulsion system. The vehicle is powered by a new topology of permanent magnet synchronous linear motor. The slider of the motor is integrally attached to the floor of the vehicle to propel. The motor is fed with an alternating voltage conveniently applied to a three-phased stator coils which are distributed in the rails that attach the vehicle travel. Therefore, the motor requires no energy storage system. A set of permanent magnets located on the slider and disposed in Halbach array, maximize thrust force. The new slider topology is able to reduce the thrust ripple, while maintaining its average value. At the same time, it reduces the normal force. The study of the dynamic behavior of electromagnetic forces concerning the movement of the slider on the stator is shown for five different topologies of the slider. A 3D Finite Element simulation tool is used.

**Keywords** - component; permanent magnet motors; linear synchronous motors; Finite element method

### I. INTRODUCTION

The transport sector, taken as a whole, i.e. including the sub-sectors automotive, aviation and maritime transport, is responsible for 23% of emissions global CO<sub>2</sub> related to the field of energy. They are the second leading cause of emissions after electricity generation [1]. Three quarters of those emissions come also from road transport: cars, trucks and buses. Thus, the use of hybrid or electric vehicles could be an improvement in terms of energy efficiency and greenhouse gases emissions, if the energy came from clean, renewable sources. Acoustic pollution also must be taken into account: 75% perceived noise in cities comes from road traffic.

According to these ideas, we propose the creation of a new bus model powered by a particular electric motor. Linear motors with direct drives are increasingly used in industrial applications even though these solutions need often more investment costs. An electric propulsion system is comprised of three main elements: power electronic converter, motor, and its controller. This paper is devoted to the linear motor selection and design. The final motor design should be obtained by constraining the material cost up a limited amount. Compared with rotary motors, the linear motors have many advantages, such as higher precision for positioning, shorter response time, better ration of actuating force to volume and without additional converting mechanism that makes the system be nonlinear, complicate and heavy [2].

Among the different types of linear electric motors, the permanent magnet synchronous linear motor (PMSLM) is

considered as the most suitable for this application; a set of permanent magnets located on the slider maximize thrust

assembly; the moving part does not have to be supplied, so the system requires no energy storage system. The motor is fed with an alternating voltage conveniently applied to a three-phased stator coils which are distributed in the rails that attach the vehicle travel; they will be supplied by sectors. Dividing the long primary into sections, the PMSLM does well in energy saving, reliability and maintenance [3]. PMSLMs although are extensively studied for levitation vehicles propulsion [2].

This work shows the study of the dynamic behavior of electromagnetic forces concerning the movement of the slider on the stator (thrust and attraction forces). Thrust ripple, determined by magnetic field, is a significant factor that affects the performance of linear motor systems. Vibration and noise of a linear motor are mainly caused by the thrust ripple, so a sinusoidal magnetic field waveform is desired; in permanent-magnet synchronous motors where the application precludes the use of a magnetic back-iron, the Halbach array produces higher torque (thrust) than the conventional array up to a certain thickness of magnets and for the same volume of magnets [4]. Halbach topology has a self-shielding property and higher flux density than vertical magnet topology [5]. The proposed Halbach arrangement in this model avoids magnetic emissions to critical areas such as the location of passengers.

In this paper a new slider structure is proposed and compared with existing ones; it has permanent magnets in Halbach array, but magnet geometry varies from conventional in order to minimize the thrust ripple and to reduce normal force. New proposal comes from a design optimization that implies the selection of the number and size of the magnets, air gap thickness or shape of the stator slots. To be an industrial application, RAMS requirements for railway applications should be taken into account [20].

Dynamic behavior of the new PMLSM in Halbach array (PMLSM-H) is compared with the behavior of the conventional PMLSM. A 3D Finite Element simulation tool is used.

## II. ELECTRIC BUS DESIGN SPECIFICATIONS

### A. General System Design

Vehicle operation is constrained to three main data: the initial acceleration, the rated cruising speed and the cruising at the maximum speed. A drivetrain capable of meeting these constraints will function adequately in the other operating regimes [6]. Refinements to these basic design constraints are necessary for an actual commercial product, but those are beyond the scope of this paper. The variables defining the design constraints are the vehicle rated velocity, the specified time to attain this velocity, the vehicle maximum velocity, the vehicle mass and other physical dimensions. The electric propulsion design variables are: 1) electric motor power rating, 2) motor rated speed, 3) motor maximum speed and 4) the extent of constant power speed range beyond the rated speed.

The electric motor can provide constant-rated thrust up to its rated speed. At this speed, as usual, the motor reaches its rated power limit. The range of the constant power operation depends primarily on the particular motor type and its control strategy. It is assumed that the electric motor operates in the constant power region beyond the nominal speed ( $v_r$ ) and up to the maximum speed. The range of operation for initial acceleration is  $0-v_r$ . For maximum acceleration, the motor operates in constant rated force:

$$F_{vr} = P_m / v_r \quad (1)$$

$P_m$  is the motor rated power. Longer constant power range of operation will lower the motor power. Minimum rated power to move vehicle mass (represented by  $M$ ) to rated speed in certain time ( $t$ ) can be established as [7]:

$$P_m = M * v_r^2 / (2 * t) \quad (2)$$

Also, the thrust force available from the propulsion system is partially consumed in overcoming the road load  $F_{RL}$ . Road load characteristics must be also taken into account.

### B. Road Load Characteristics

The road load,  $F_{RL}$ , consists of rolling resistance force ( $F_{rod}$ ), aerodynamic drag force ( $F_{rad}$ ) and climbing resistance ( $F_{rpnd}$ ) [6-7]:

$$F_{RL} = F_{rod} + F_{rad} + F_{rpnd} \quad (3)$$

The rolling resistance is caused by the tire deformation on the road:

$$F_{rod} = f_r * M * g \quad (4)$$

$f_r$  is the tire rolling resistance coefficient; it increases with vehicle velocity and also during vehicle turning maneuvers;  $g$  is the gravitational acceleration constant. Aerodynamic drag is the viscous resistance of air acting upon the vehicle:

$$F_{rad} = \frac{1}{2} * \xi * CD * A * v^2 \quad (5)$$

$\xi$  is the air density,  $CD$  is the aerodynamic drag coefficient,  $A$  is the vehicle frontal area and  $v$  is the vehicle speed in addition to the head-wind velocity. The climbing resistance (positive  $F_{rpnd}$ ) and the downgrade force (negative  $F_{rpnd}$ ) is given by:

$$F_{rpnd} = M * g * \sin \alpha \quad (6)$$

where  $\alpha$  is the grade angle.

### C. Motor Selection

Linear motor will be designed contained to the following electric bus data; a commercial bus model is selected [7]:

- 0–13.88 m/s in 12 s;
- Vehicle mass of 18.000 kg;
- Frontal area: 9 m<sup>2</sup>
- Rolling resistance coefficient of 0.013;
- Aerodynamic drag coefficient of 0.29;

Following assumptions are made in the design: rolling resistance independent of velocity, zero head-wind velocity and level ground.

According to eq. (2), the minimum power for the motor to reach 13.88 m/s in 12 seconds is 144,5 kW. The road load force results 2619,54 N. The global motive force  $F$  required to the propulsion system is  $F=12,9$  kN on level ground. The motor power given is 180 kW.

PMLSMs have an attractive force produced between the magnets on board and the stator iron yoke on the ground. It must be considered in the final motor design.

## III. PMLSM-H FORCE ANALYSIS

In order to maximize the thrust force, stator coils have ferromagnetic core, so the PMLSM-H operates in attractive mode. Slider consist of five permanent magnets in Halbach array The longitudinal cross section of the PMLSM-H is shown in Fig. 1.

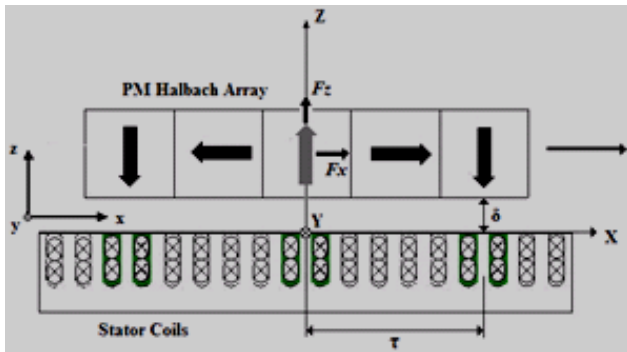


Fig. 1. Longitudinal cross section of a long stator PMLSM-H

The slider moves at a synchronous speed in a stationary coordinate system [2]:

$$v = v_s = 2\tau f_s = \frac{\omega}{\pi} \tau \quad (7)$$

$f_s$  are the stator voltage frequency and  $\tau$  are the pole pitch. Thrust may be represented by an analytic formula. It can be obtained by solving the multiboundary-value field problem. From the magnetic vector potential (MVP) transfer matrix method [4] results:

$$F_x = k_{F0}(\delta) I_1 \sin\left(\frac{\pi}{\tau} x_0\right) \quad (8)$$

$k_{F0}$  is the coefficients of thrust force regarding the motor structure parameters,  $I_1$  the effective armature current;  $\tau$  the pole pitch,  $\delta$  the air-gap length and  $x_0$  the mechanical load angle. Electromagnetic thrust ripple is a form of oscillation causing vibration, noise, complicates the design and operations of the system control.

It has been verified that the Halbach arrangement (with respect to the vertical magnets), reduces the "stress" of the magnets themselves and concentrates most of magnetic flux in the air gap. Fig. 2 shows the model and concentration of magnetic flux in the air gap.

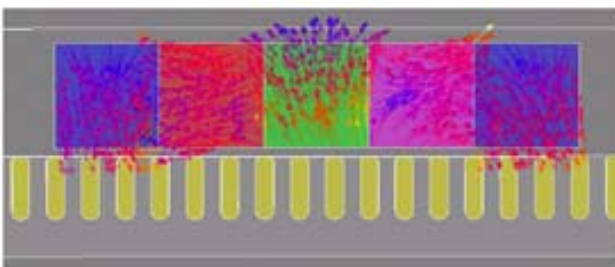


Fig. 2. Magnetic flux of PMLSM with Halbach array

#### IV. PRELIMINARY PMLSM-H MODELS

##### A. Mechanical Design

Fig. 3 shows the device in which the PM slider is housed; it will severally bound to the lower structure of the vehicle; includes small wheels that would be used only if the vehicle wheels pricked; these small wheels would avoid the PMSLM deteriorate by the blow. This structure protects the magnets from of obstacles in the road. The magnets design and proper installation on the vehicle take to the selection of four 45 kW PMLSM-H instead of designing a single larger 180 kW motor. Four motors are located in the lower housing of the bus as shown in Fig. 4.

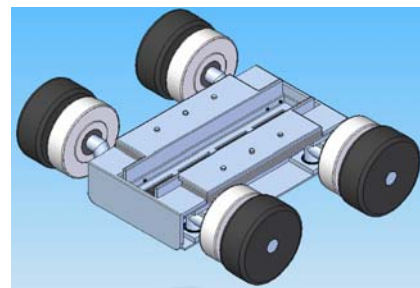


Fig. 3: Structure housing of the PMSLM slider

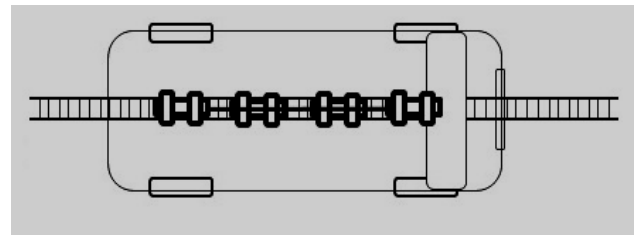


Fig. 4: Location of four PMSLMs in the bus housing

##### B. Model of PMLSM-H with adjusted magnet width (PMLSM-H1)

The initial PMLSM is obtained preliminary from a 45 kW rotary model and using different design recommendations for synchronous linear motors; linear synchronous model is redesigned by Finite Element method (FEM) Flux™ program. For the short secondary type of PMLSM, the detent force can be reduced by changing the magnet width to the slot pitch. Some research works [8] show that detent force when magnets are in Halbach array takes a minimum value when mentioned ratio is  $(1.18+0.47*n)$ , where  $n$  is integer. Results are confirmed in this particular PMLSM design. For  $n=4$ , the relation between magnet width to the slot pitch reaches a value of 3.06. The result is that flux density of the Halbach topology is stronger by more than 41% than with conventional array as same as air-cored PMLSM.

Adapting this method to the PMLSM-H proposed the initial model PMLSM-H1 is derived; large air gap length is

used, as recommended for road transport applications [3]. In the first column of Table I motor parameters (PMLSM-H1) are shown.

C. Model of PMLSM-H with inclined magnets (PMLSM-H2).

To reduce thrust ripple in PMLSMs with vertical magnet topology several methods have been reported by many researchers [9]–[19]. These methods are achieved either by an adequate control of the driver [9-11] or by special motor design [12-19]. Wherein the methods used at the design stage can be skewing and optimally disposing the magnet [12-13].

Fig. 4 shows the proposed PMLSM with Halbach array where magnets are conveniently skewed (PMLSM-H2). We first analyze the forces for those PMLSMs types using FEM. Taking into account PMLSM-H2 configuration, thrust force is calculated by FEM for different air-gap dimensions and skew angles. For the numerical model by FEM Flux™ software is used.

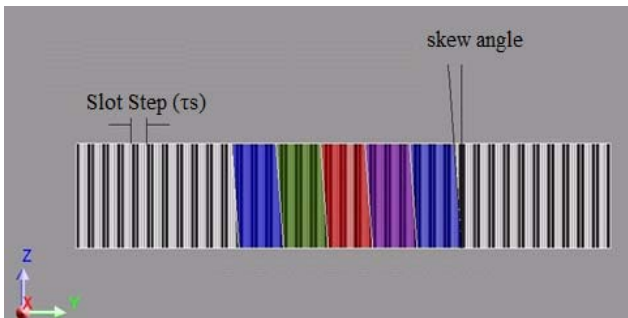


Fig. 4. PMLSM-H2 topology: Halbach array with skewed magnets.

TABLE I – MAIN PARAMETERS OF PMLSM-H1 AND H2

Description	PMLSM -H1	PMLSM-H2
<b>Stator (mm):</b>		
Length	997	997
Depth	140	140
Yoke's Height	59	59
Slot's Width	10,6	10,6
Slot pitch (τs)	20,55	20,55
Air-gap length (mm)	20	20
<b>Translator (mm):</b>		
Length	314,49	314,49
Height of Magnets	63,55	63,55
Width of Magnets	62,89	62,89
Pole pitch	125	125
Skew	0	(1/2-3/2)*τs

D. Simulation results for PMLSM-H1 and PMLSM-H2 models.

A three phase current system was applied to the models; current density was 3 A/mm<sup>2</sup>. Fig. 5 shows thrust force for different skew angles from 0° (corresponding to PMLSM-H1) to 3/2 τs. Thrust ripple amplitude depends on the

number of harmonics in the field created by the magnets (in the gap) and in the field created by the current, which depends on the characteristics of the winding and temporary own current harmonics. These results shows that magnet inclination does not improves thrust force magnitude, as expected. For PMLSM-H1 fig. 5 shows thrust force with a medium value of 8.5 kN (0.38 kN ripple). Thrust ripple also varies with magnet skew; minimum ripple (fig. 6) is obtained with τs skew angle (0,33 kN), that is 4,3% of rated thrust; although thrust force reduces 13% (to 7,51 kN). Optimum magnet skew angle has been calculated to obtain a suitable thrust to ripple ratio. It was found that 3τs/4 skew maximizes mentioned relation.

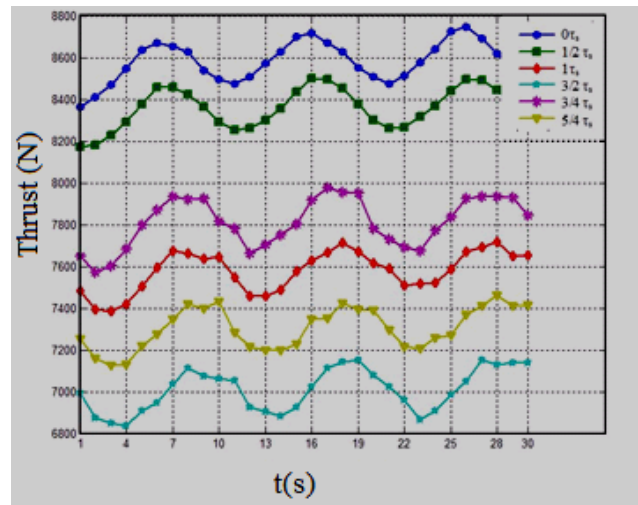


Fig.5. Thrust force for PMLSM-H1 and H2 for magnet skew angles from 0 to 3τs/2.

Normal force (attraction force) increases with magnet skew as shown in fig. 6; it is exerted on the active surface area of each of the magnets of the slider. Normal force mean value for PMLSM-H1, 4,12 kN results less than 50% of the thrust force, low than usual, because of the high air-gap length (20 mm) recommended for road transport application.

Simulations were also made to study the effect of the air-gap length; PMLSMs with Halbach array with 5 mm to 30 mm air-gap were analyzed. The thrust force of these motors, for variable magnet skew is shown in fig. 7. Thrust force reduces with the increasing air-gap length, as expected; for each air-gap length variation, thrust ripple changes with the skew angle; optimal skew angle is different in each case.

Once those results are analyzed, a shape change in the magnets design is proposed, in order to improve obtained thrust with minimum thrust ripple. Diverse slider topologies are studied and compared with PMLSM-H1 and PMLSM-H2 model results.

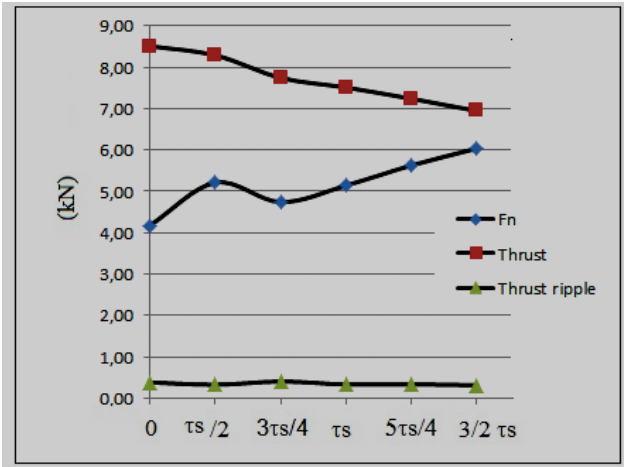


Fig. 6. PMLSM-H2. Normal force, thrust force and ripple vs skew angle

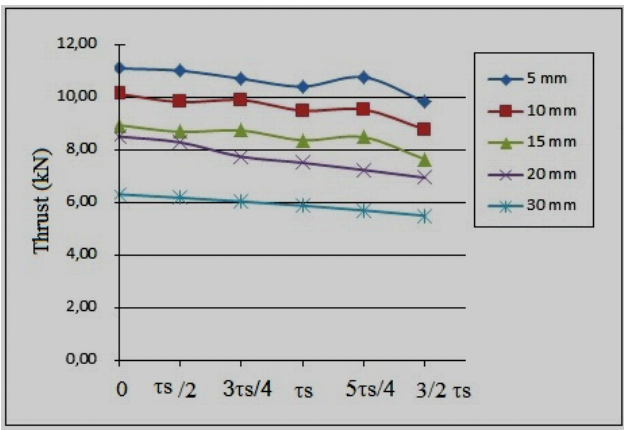


Fig. 7. Thrust force for PMLSM-H for magnet skew and variable air-gap length

Results obtained by finite element simulation should be contrasted by experimental tests. The initial Halbach motor model was contrasted with a similar motor with less power that has been experimentally contrasted [8]. Flux density or magnetic field distribution results were similar to those published in [8]

V. NEW SLIDER TOPOLOGIES

In order to improve obtained thrust force with minimum thrust ripple, a change in the magnets design is proposed. Three new slider geometries are designed and analyzed, PMSLM-H TYP-7, MSLIP-H TYP-L and PMSLM-H TYP-C topologies; names given to those new topologies are related with the shape of each of the magnets that conform the slider. 3D Model and YZ slider view is represented for each topology in figs. 8, 9 and 10. Stator dimensions are the same as the previous model (Table I). A three phase current system was applied to the models; applied current density was 3 A/mm<sup>2</sup>.

Different values of skew were tested for each topology; in the all cases best result was obtained with τs/2 skew

angle. Table II shows 3-D FEM results of thrust and ripple for three mentioned new topologies for τ/2 skew angle.

TABLE II  
RESULTS FOR FIVE PMSLM-H TOPOLOGIES

PMSLM Topology	Thrust (N)	Ripple (N)	% Ripple	Normal Force (N)
"H1"	8501,4	382,8	4,50	4120,8
"H2"(τs)	7512,5	332,5	4,43	5140,2
"TYP-7"	8082,2	274,2	3,39	1766,3
"TYP-L"	8140,2	268,8	3,30	1602,2
"TYP-C"	5627,6	520,6	10,8	2190,1

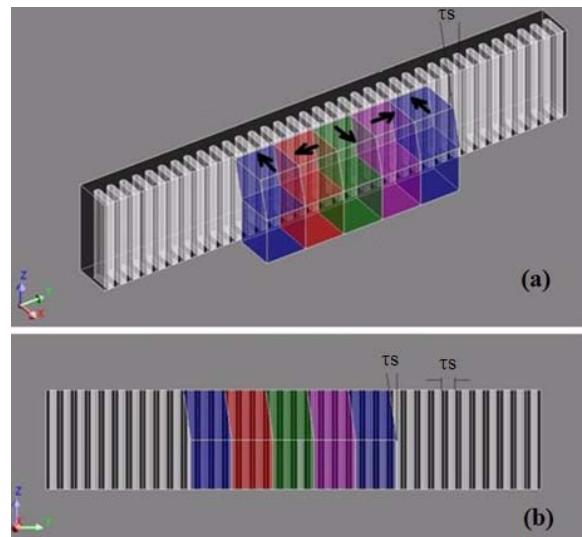


Fig. 8. PMSLM-H TYP-7. (a) 3D Model, (b) YZ slider view

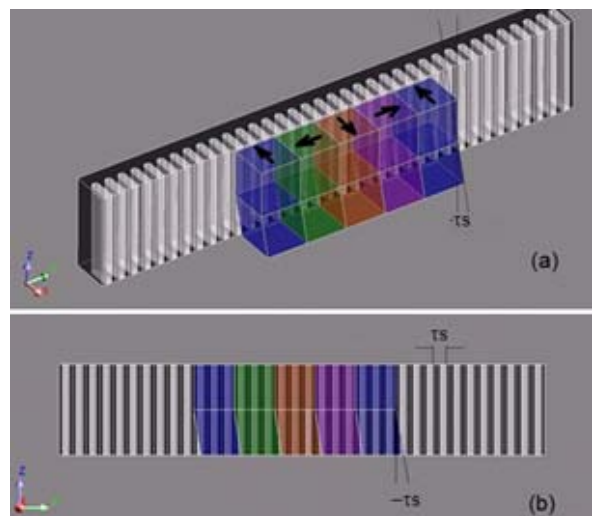


Fig. 9. PMSLM-H TYP-L. (a) 3D Model, (b) YZ slider view

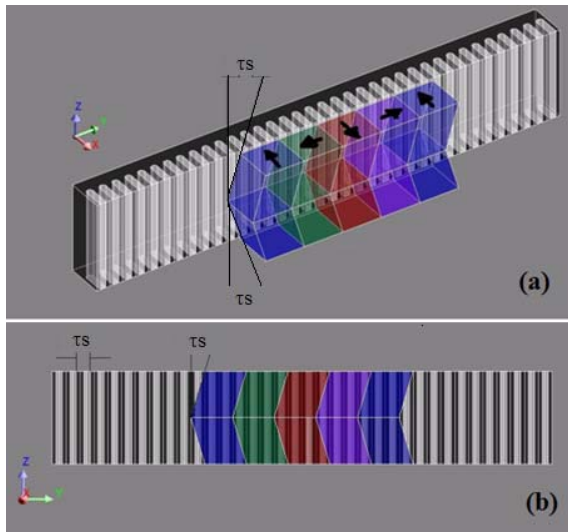


Fig. 10. PMSLM-H TYP-C. (a) 3D Model, (b) YZ slider view

As shown (Table II), maximum thrust (8.5 kN) is obtained with the PMSLM-H topology.

The PMSLM-H TYP-C topology doesn't improve the thrust force, increasing its corresponding ripple and the normal force. It is not considered as a good proposal.

On the other hand, the PMSLM-H TYP-L offers reduced thrust ripple (0.27 kN). The proposed new topology PMSLM-H TYP-L also gets the best thrust to ripple ratio; the normal attractive force between the armature and slider results less than 20% of thrust force due to the large air-gap length required for the application and the new flux distribution imposed by the new slider. Normal force is reduced more than 50% compared to classical topology PMSLM-H1. Fig. 11 shows thrust force for PMSLM-H TYP-7 and PMSLM-H TYP-L models, 20 MM air-gap length.

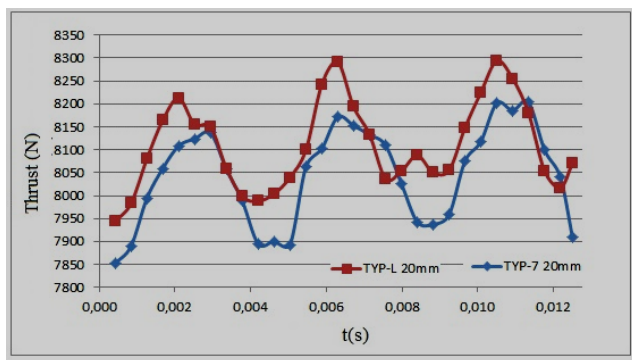


Fig. 11. Thrust force for PMSLM-H TYP-7 and PMSLM-H TYP-L

## VI. OTHER CONSIDERATIONS

The final motor design should be a compromise between several quantities, as for example, the efficiency and the

cost; both must be combined to form an objective function. If the motor has several distinct working points, diverse optimizations for each point must be made. The final motor design will be a compromise between these optimizations by favoring the one corresponding to the nominal working point of the motor.

Fig. 12 represents flux density obtained for PMSLM-H TYP-L model.

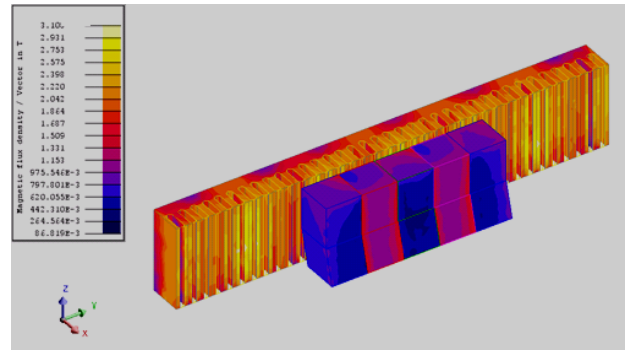


Fig. 12. Flux density for PMSLM-H TYP-L

## VII. CONCLUSIONS

A new topology of Permanent Magnet Linear Synchronous Motor (PMSLM) is proposed. The PMSLM in Halbach array is initially designed to propel a wheeled vehicle; a long stator of ferromagnetic material is used, so the normal force is large and attractive. The proposed PMSLM-H TYP L topology minimizes the attraction force and maximizes thrust, maintaining minimum thrust ripple. The advantage of the proposed motor is that combines a high thrust force (thanks to the Halbach arrangement of the magnets of the slider), and a reduced normal force and thrust ripple. Performance motor evaluation for a 45 kW is accounted by FEM. Two new topologies have been designed to obtain a suitable thrust to ripple ratio. The best of the new proposed topologies, named PMSLM-H TYP-L offers high thrust with reduced thrust ripple. Normal force is reduced more than 50% compared to classical topology PMSLM-H1. Thrust ripple is reduced to 3.3% of rated thrust. Therefore, the proposed motor is very promising for high-thrust applications. The final motor design should be a compromise between several quantities, as for example, the efficiency and the cost.

## REFERENCES

- [1] IEA. World Energy Outlook. 2015
- [2] J. F. Gieras and Z. J. Piech, Linear Synchronous Motors Transportation and Automation Systems. Electric Power Engineering Series, 1999.
- [3] Liyi Li, Junjie Hong, Hongxing Wu, Zhe Zha and Xiaopeng Li "Adaptive Back-stepping Control for the Sectioned Permanent Magnetic Linear Synchronous Motor in Vehicle Transportation System" IEEE Vehicle Power and Propulsion Conference (VPPC), September 3-5, 2008, Harbin, China.

- [4] J. Ofori-Tenkorang, J. H. ILang. A Comparative Analysis of Torque Production in Halbach and Conventional Surface-Mounted Permanent-Magnet Synchronous Motors. Industry Applications Conference, Thirtieth IAS Annual Meeting, IAS '95. pp. 657 - 663 vol.1 1995.
- [5] J. Ofori-Tenkorang, J. H. ILang. A Comparative Analysis of Torque Production in Halbach and Conventional Surface-Mounted Permanent-Magnet Synchronous Motors. Industry Applications Conference, Thirtieth IAS Annual Meeting, IAS '95. pp. 657 - 663 vol.1 1995.
- [6] D. L. Trumper, W. J. Kim, and M. E. Williams, "Design and analysis framework for permanent-magnet machines," IEEE Trans. Ind. Appl., vol. 32, pp. 371-379, Apr. 1996.
- [7] Automotive Handbook. Germany: Robert Bosch GmbH, 1986.
- [8] Mehrdad Ehsani, Khwaja M. Rahman, Hamid A. Toliyat, "Propulsion System Design of Electric and Hybrid Vehicles". IEEE Transactions On Industrial Electronics, Vol. 44, No. 1, February 1997
- [9] Seok-Myeong Jang , Sung-Ho Lee, and In-Ki Yoon. Design Criteria for Detent Force Reduction of Permanent-Magnet Linear Synchronous Motors With Halbach Array. IEEE Trans. On Mag. VOL. 38, NO. 5, Sept. 2002
- [10] C. Rohrig and A. Jochheim, "Identification and Compensation of Force Ripple in Linear Permanent Magnet Motors," Proceedings of American Control Conference, 2001, Vol. 3, pp. 2161-2166.
- [11] J.Y. Hung, Z Ding, "Design of currents to reduce torque ripple in brushless permanent magnet motors," IEE Proceedings of Electric Power Applications, July 1993, Vol. 140, Issue: 4, pp. 260 -266.
- [12] Martinez G., Atencia J., Martinez-Iturralde M., Garcia Rico A., Flhez J. Reduction of detent force in flat Permanent Magnet Linear Synchronous Machines by means of three different methods. Proceedings of the IEEE International Electric MACHines and Drives Conference (IEMED,2003), Wisconsin, USA, 2003.
- [13] I. S. Jung, J. Hur, D. S. Hyun, "Performance analysis of skewed PM linear synchronous motor according to various design parameters," IEEE Trans. on Magnetics, Vol. 37 Issue 5, pp. 3653 -3657. Sept. 2001
- [14] Zhang Ying, ChenYou-ping, AIWu, Zhou Zu-de. Design strategy for detent force reduction of permanent magnet linear synchronous motor J Shanghai Univ (Engl Ed), 2008, 12(6): 548-553
- [15] T. Yoshimura, H. J. Kim, M. Watada, S. Torii, D.Ebihara, Analysis of the reduction of detent force in a permanent magnet linear synchronous motor, IEEE Tr. on Mag., Nov. 1995, Vol. 31, 6, pp.3728 -30.
- [16] Z. O. Zhu, Z. P. Xia, D. Howe, P. H Mellor, "Reduction of cogging force in slotless linear permanent magnet motors," IEE Proceedings of Electric Power Applications, July 1997, Vol. 144, Issue 4, pp. 277 -282.
- [17] Inoue M., Sato K., "An approach to a suitable stator length for minimizing the detent force of permanent magnet linear synchronous motors," IEEE Transactions on Magnetics, July 2000, Vol. 36 Issue: 4, pp. 1890 -1893. Vol. 44, No. 3, March 2008
- [18] Liu, Zhengmeng; Zhao, Wenxiang; Ji, Jinghua; et ál."A Novel Double-Stator Tubular Vernier Permanent-Magnet Motor With High Thrust Density and Low Cogging Force" IEEE Transactions on Magnetics Vol. 51, Number 7 , Jul. 2015
- [19] Miyamoto, Yasuhiro; Tanabe, Masahiko; Higuchi, Tsuyoshi; et ál. "Improvement of Cogging Thrust in Permanent-Magnet-Type Linear Synchronous Motors" Electrical Engineering in Japan. Vol.: 191, Number 1. pp: 50-58. April 2015
- [20] Batelaan, Justin "A linear motor design provides close and secure vehicle separation of many transit vehicles on a guideway "IEEE Transactions on Industrial Electronics. Volume: 54 Issue: 3. pp: 1778-1782 . June 2007.